ISSN 1061-9348, Journal of Analytical Chemistry, 2024, Vol. 79, No. 6, pp. 680–689. © Pleiades Publishing, Ltd., 2024.

ARTICLES

A Voltammetric Sensor Based on a Chitosan, Graphitized Carbon Black, and Molecularly Imprinted Polyarylene Phthalide Composite for Clarithromycin Detection

Yu. A. Yarkaeva[a], *, M. I. Nazyrov[a], D. A. Dymova[a], and V. N. Maistrenko[a], †

[a] *Faculty of Chemistry, Ufa University of Science and Technology, Ufa, 450076 Russia*

**e-mail: julijajarkaeva05@gmail.com*

Received April 13, 2023; revised April 27, 2023; accepted April 27, 2023

Abstract—A voltammetric sensor based on a glassy carbon electrode modified with a chitosan, Carboblack C graphitized carbon black, and molecularly imprinted polyarylene phthalide composite is developed for the selective detection of antibiotic clarithromycin. The polyarylene phthalide used for modification contains diphenylenethio- and diphenylene oxide fragments in a 1 : 2 ratio in the main polymer chain. Clarithromycin-imprinted polyarylene phthalide was obtained using the phase inversion method. The composition and morphology of the modifying coating were investigated by IR spectrometry and scanning electron microscopy. The electrochemical and analytical characteristics of the sensor were investigated by electrochemical impedance spectroscopy, cyclic voltammetry, and differential pulse voltammetry. Optimal conditions for recording the analytical signal were selected. Using $[Fe(CN)_6]^{3-/4-}$ as a probe, the linear range of the detected concentrations was found to be 1×10^{-7}–5×10^{-4} M with a limit of detection of 5.3×10^{-8} M. Using a clarithromycin-imprinted polymer enhances the sensor sensitivity by nearly tenfold compared to the nonimprinted polymer. The proposed sensor was tested using urine, blood plasma, and various food samples (meat, milk), the recovery values were 90–96, 80, and 92%, respectively, with relative standard deviations not exceeding 10% in all cases.

Keywords: molecularly imprinted polymers, polyarylene phthalide, phase inversion, voltammetric sensor, clarithromycin, graphitized carbon black

DOI: 10.1134/S1061934824700059

Molecularly imprinted polymers (MIPs) are synthetic analogues of natural biological systems, such as antibody–antigen interactions, functioning by the principle of a "lock and key" mechanism. MIPs exhibit specificity and selectivity akin to biological receptors, while offering advantages, such as physical robustness, reliability, resistance to high pressure and temperature, inertness to various chemical substances, stability, prolonged storage under ambient conditions, and cost-effectiveness [1, 2]. Natural receptors typically require storage at low temperatures, whereas MIPs can be stored for extended periods without specific storage conditions, and can be utilized over a much broader range of temperatures and pH levels. The growing interest in the design, development, and application of MIPs in recent years underscores the importance of this field in chemical sensing. MIP-based sensors are employed for analyzing food products, environmental samples, and biological specimens due to their high sensitivity, specificity, and stability [2].

In the creation of MIP-based sensors, the conventional method typically involves the polymerization (chemical, electrochemical, photopolymerization) of monomer molecules in the presence of a template, followed by its removal from the polymer, resulting in cavities complementary in size, shape, and molecular interactions to the template [3–5]. However, alternative methods for obtaining MIPs are known, such as the phase inversion method and soft lithography [1, 6]. The latter involves the fabrication of a stamp composed of a self-organizing template layer, which is pressed into a partially polymerized film and held until complete polymerization, after which the stamp is removed by washing with an appropriate solvent. This approach is typically employed for the detection of large molecules and structures that cannot be uniformly distributed throughout the polymer volume, for instance, in the detection of *Escherichia coli* cells [7]. The phase inversion method involves the utilization of pre-existing polymers, which are precipitated onto the surface of a working electrode from a solution in the presence of a template by adding another solvent that induces the precipitation of the

† Deceased.

template-containing polymer (wet phase inversion) [8, 9], or by solvent evaporation from the polymer upon heating or centrifugation (dry phase inversion) [1]. Its primary advantage lies in its simplicity and rapid fabrication of MIP-based sensors. A solvent compatible with both the base polymer and the template is used for dissolving components, allowing the formation of "guest–host" complexes in the solution. The dry phase inversion method is simpler and more convenient compared to wet phase inversion, as it does not require the use of a second solvent. Typically, it is implemented by heating a polymer precipitated on an electrode surface. MIPs obtained through solvent evaporation possess a dense and a homogeneous structure due to the gradual increase in the polymer concentration in the forming film as a result of solvent evaporation [10].

The phase inversion method was developed by Kobayashi et al. in 1996 [11]. Since then, MIPs obtained by phase inversion have been applied in enantiomeric separation [12], solid-phase extraction [13], and the detection of various compounds in food products and aqueous media [14, 15]. The preparation of MIPs via phase inversion typically lacks a cross-linking process, which in certain cases may lead to the collapse of cavities during template removal. However, this method offers the simplest means for obtaining thin-film MIPs, essential for the fabrication of voltammetric sensors. Publications on the creation of electrochemical sensors with MIPs obtained via the phase inversion method are rather limited [9, 16–18].

Phase inversion is employed in the fabrication of MIPs based on polymers, such as polysaccharides (dextran, chitosan, cellulose) [17, 19], polyamides (nylon) [18], acrylic copolymers [9, 16, 20], polyethylene copolymers [21], aromatic polysulfones [22], etc. Polyarylene phthalides (PAPs) are also of interest for the fabrication of MIP sensors; the PAP thin films exhibit electrical conductivity and chemical resistance to heating and aggressive media. Polyarylene phthalides have previously been studied and utilized for the fabrication of sensors based on composite materials [27]. Application of a polymer onto the electrode surface often leads to decreased currents due to increased resistance; therefore, components enhancing electrical conductivity must be added to the sensor layer. Lately, nanomaterials such as Au and Pt nanoparticles, single-walled and multi-walled carbon nanotubes, and reduced graphene oxide [5, 26, 28] have been used for these purposes among others.

The primary characteristic of MIP sensors is the selectivity of binding to the target molecule. i.e., the template molecule. Typically, selectivity (also referred to as the selectivity coefficient or imprinting factor, F_{imp}) is evaluated as the ratio of binding efficiencies of the template with the MIP and the nonimprinted polymer (NIP), derived from analytical signals (often from sensitivities: $F_{imp} = S_{MIP}/S_{NIP}$).

Another advantage of MIPs is their universality, which lies in the fact that the template can be any substance with specific functional groups, ranging from relatively small molecules, such as amino acids, to larger molecules like antibiotics, proteins, and even subcellular forms (phages and viruses) and cells. MIP sensors are most commonly used for detecting enantiomers of biologically active compounds and antibiotics [1, 2]. Antibiotics detection is an essential applied task in analytical chemistry because of their wide application and, consequently, their widespread presence in the environment and food products. Among them, macrolides represent a group of antibiotics widely used in medicine for treating various diseases, but their most important application is the treatment of respiratory infections, including the treatment of patients with COVID-19. They are also used in veterinary medicine. Widely used macrolides, such as erythromycin, azithromycin, and clarithromycin (Clr), are often detected in the environment and food products, leading to the development of antibiotic resistance in living organisms. Previously, electroanalytical methodologies have been developed for the detection of macrolides based on the use of various electrochemical (bio)sensors [29].

In this study, we present a voltammetric sensor based on a glassy carbon electrode (GCE), modified with a composite of chitosan (CHT), graphitized carbon black Carboblack C (CB), and molecularly imprinted polyarylene phthalide (PAP) obtained by the phase inversion method, for the selective detection of clarithromycin. The used PAP contains diphenylthio- and diphenylenoxide fragments in a 1 : 2 ratio in the main polymer chain [27]. Surface morphology was investigated by scanning electron microscopy (SEM), and the composition of the modifying coating was examined studied by IR spectrometry. The electrochemical and analytical characteristics of the sensor were studied by electrochemical impedance spectroscopy (EIS), cyclic voltammetry (CV), and differential pulse voltammetry (DPV). Optimal conditions for the detection of clarithromycin using the proposed sensor were selected. A solution of $[Fe(CN)_6]^{3-/4-}$ was employed as a probe for clarithromycin detection. The proposed sensor was validated using real samples of biological fluids (urine and blood plasma) and food products (meat, milk). The reproducibility, stability, and selectivity of the sensor were investigated.

EXPERIMENTAL

Reagents and equipment. Clarithromycin (≥99.5%), azithromycin (≥99.5%), lincomycin (≥99.5%), $K_3Fe(CN)_6$ (≥99.0%), and $K_4Fe(CN)_6$ (≥99.0%) were purchased from Sigma-Aldrich (United States), and graphitized carbon black powder

Carboblack C was acquired from Restek (United States). Samples of a polyarylene phthalide polymer (≥99%) were provided by the Laboratory of Functional Polymer Synthesis at the Ufa Institute of Chemistry of the Russian Academy of Sciences (Russia). A phosphate buffer solution (PBS, KH_2PO_4 + Na_2HPO_4, 0.1 M, pH 6.86) was used as a supporting electrolyte for clarithromycin, while a 0.1 M KCl solution served as a supporting electrolyte for $[Fe(CN)_6]^{3-/4-}$. A 5 mM solution of $[Fe(CN)_6]^{3-/4-}$ was employed as a probe for clarithromycin detection.

All electrochemical measurements were conducted using an Autolab PGSTAT 204 potentiostat-galvanostat with an FRA32M impedance module (Metrohm Autolab, Netherlands) equipped with NOVA software. The standard three-electrode cell consisted of a modified glassy carbon electrode (Metrohm Autolab, Netherlands) of a diameter of 3 mm as a working electrode, a platinum plate as an auxiliary electrode, and a silver–silver chloride electrode with a 3.5 M KCl solution as a reference electrode. The pH of the solutions was measured using a Seven Compact pH/Ion S220 pH meter (Mettler-Toledo, Switzerland). Solutions were mixed with an MR Hei-Tec magnetic stirrer (Heidolph, Germany). IR-spectra were recorded in the range 450–3500 cm^{-1} using an FTIR-8400S spectrometer (Shimadzu, Japan) at room temperature (resolution 8 cm^{-1}, number of scans 30) using the IR Solution software. SEM images were obtained using a Tescan Mira scanning electron microscope (Tescan, Czech Republic).

Electrode modification. To modify the glassy carbon electrode, 1 mL of a chitosan solution was combined with 2 mg of Carboblack C, and the mixture was sonicated in an ultrasonic bath for 40 min until a homogeneous dispersion was obtained. The chitosan solution was selected for dispersing carbon black because it forms the most stable and homogeneous dispersion compared to other solvents (dimethylformamide (DMF), chloroform, acetone, ethanol). An aqueous chitosan solution was prepared by dissolving 0.0100 g in 5 mL of deionized water. A deagglomerated suspension based on 0.3 μm Al_2O_3 and a specialized polishing material (Allied High Tech Products, United States) was used for electrode surface polishing. For electrode surface modification, 3 μL of Carboblack C dispersion was applied using a drop-casting method and dried under an infrared lamp to complete drying.

To prepare a polymer–template mixture, 10 mg of a polymer and 4 mg of clarithromycin were dissolved in 1 mL of dimethylformamide (DMF). The optimal polymer-to-template ratio was determined experimentally based on the values of I_p and the relative standard deviation (RSD). To obtain a MIP on the surface of CB–CHT/GCE, 1 μL of the obtained polymer–template solution was applied using a drop-casting method, dried under an IR lamp for 3 min, and the template was removed by treating with a 1 M solution of H_2SO_4 for 90 s with stirring. A 1 M solution of H_2SO_4 was selected as the optimal solvent for template removal based on the values of I_p and RSD. A sensor with nonimprinted PAP (niPAP) was prepared using a similar method but without the addition of the template.

Procedure. Differential pulse voltammetry (DPV) curves of $[Fe(CN)_6]^{3-/4-}$ were recorded over a potential range from 0 to 0.6 V with a pulse amplitude of 0.025 V, pulse width of 0.05 s, interval time of 0.25 s, and scan rate of 25 mV/s. Electrochemical impedance spectra were recorded over a frequency range from 100 kHz to 0.1 Hz with an amplitude of 5 mV. Cyclic voltammetry (CV) curves of $[Fe(CN)_6]^{3-/4-}$ were measured over a potential range from –0.1 to 0.6 V at a potential scan rate of 0.1 V/s. Before recording the DPV curves, the sensor was immersed in an analyte solution for 40 s to accumulate clarithromycin. All measurements were conducted at 25 ± 0.1°C.

Preparation of solutions. A 0.5 mM clarithromycin solution was prepared by dissolving an accurately weighed portion of the reagent in 25 mL of a phosphate buffer solution (PBS). Solutions of lower concentrations were prepared by successive dilutions. Urine samples were obtained from a healthy donor, while blood plasma was acquired from the Ufa Republican Blood Transfusion Station. Urine and blood plasma samples (2.5 mL each) were centrifuged for 5 min and diluted by 10 times in PBS with a pH of 6.86. Known amounts of clarithromycin were added to the diluted samples to obtain solutions with concentrations of 5.0 and 0.6 μM, respectively.

A sample of ground beef was prepared as follows. A 10-g portion of ground beef was mixed with 10 mL of PBS containing 0.1 μM of clarithromycin. The mixture was then subjected to extraction in a thermostat at 37 ± 1°C for 90 min, followed by incubation at 65 ± 1°C for 30 min. Afterwards, the sample was centrifuged for 20 min at 3000 rpm [30].

For the milk sample, we took 10 mL of milk (2.5% fat) and diluted it with 10 mL of PBS containing 0.5 μM of clarithromycin [30].

Ultrapure deionized water with a specific conductivity of 0.1 μS/cm was used to prepare all solutions.

RESULTS AND DISCUSSION

The surface morphology of the electrodes at each modification stage was studied by scanning electron microscopy. Upon the deposition of the chitosan and carbon black composite onto the GCE surface, an uneven layer formed, consisting of partially agglomerated Carboblack C particles with sizes up to 10 μm (Fig. 1a). At higher resolution (Fig. 1b), individual spherical Carboblack C particles with sizes ranging from 0.2 to 0.5 μm were observed. Upon the deposition of the polyarylene phthalide onto the CB–CHT-modified surface of the electrode followed by drying under an IR lamp, a dense and a uniform film with

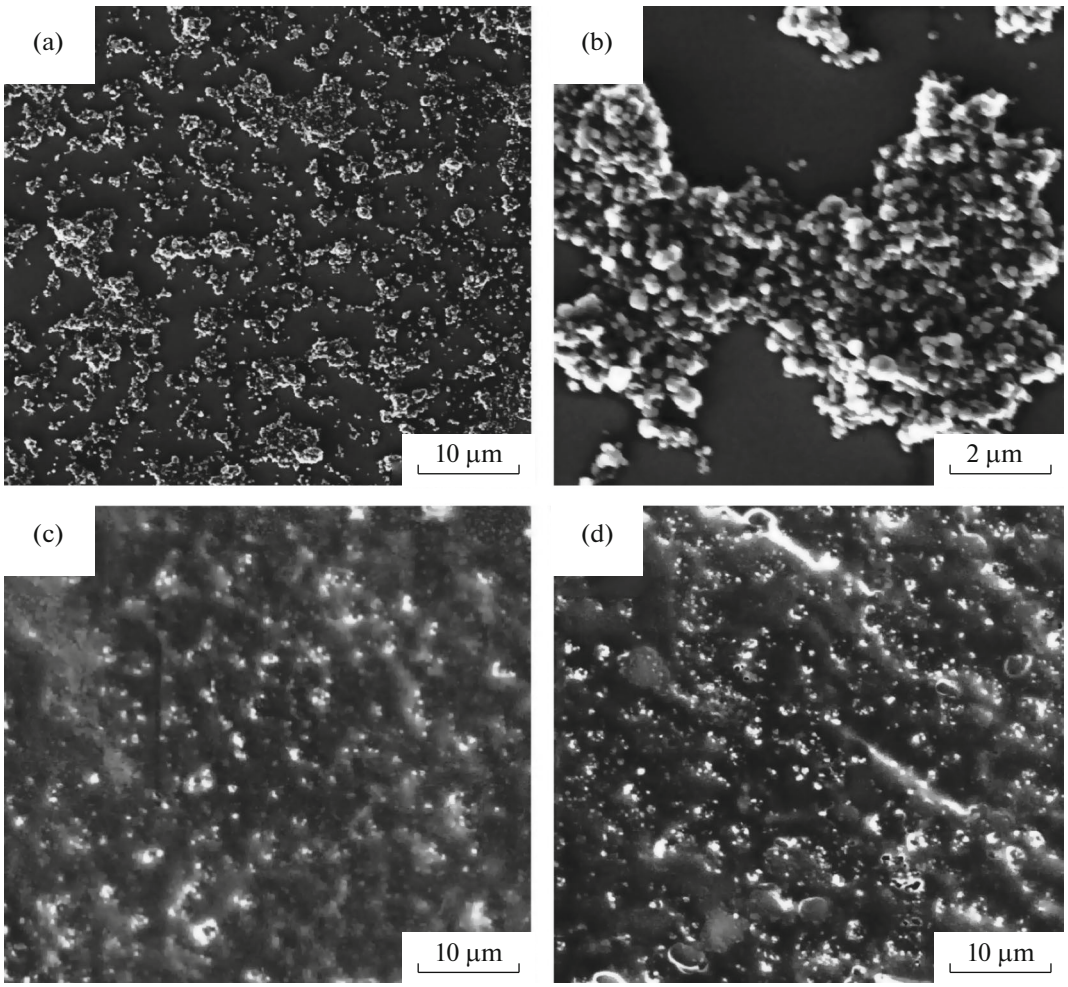

Fig. 1. SEM images of (a, b) CB–CHT/GCE, (c) PAP/CB–CHT/GCE, and (d) miPAP/CB–CHT/GCE.

small irregularities formed (Fig. 1c). This confirms that MIPs obtained by solvent evaporation have a dense and a homogeneous structure due to the gradual increase in polymer concentration in the forming film. After the removal of the template from the polymer and the formation of molecularly imprinted polyarylene phthalide (miPAP), surface roughness increased due to the formation of pores.

The IR spectra confirmed the presence of clarithromycin in the PAP film. Figure 2 shows IR spectra of Carboblack C, CB–CHT composite, PAP, clarithromycin, and PAP before template removal. In the Carboblack C spectrum, there are minimal absorption bands, except for slight stretching vibrations at 1640 cm^{-1}, corresponding to C=C bonds [28]. In the spectrum of the CB–CHT composite, characteristic peaks at 1647 and 1618 cm^{-1} correspond to stretching vibrations of C=O from –NHCO– and bending vibrations of the $-NH_2$ group. Bands of stretching vibrations of C–H and C–N are at 2921 cm^{-1}, N–H in-plane vibrations of –NHCO– are at 1377 cm^{-1}, and C–O–C bands are observed at 1070 cm^{-1} [31]. The characteristic bands in the PAP spectrum are at 1767 cm^{-1}, corresponding to the phthalide group; 727 cm^{-1}, corresponding to the Ar–S–Ar group; and 1244 cm^{-1}, corresponding to the Ar–O–Ar group. The characteristic bands in the clarithromycin spectrum are detected at 1732 cm^{-1}, corresponding to the carbonyl group of the lactone, and at 1170 cm^{-1}, corresponding to the C–O vibration in the lactone. These bands can be seen in the spectra of the PAP film with the template, confirming the presence of clarithromycin.

The electrochemical characteristics at each stage of electrode modification were investigated by cyclic voltammetry (Fig. 3a) and electrochemical impedance spectroscopy (Fig. 3b) with the standard $[Fe(CN)_6]^{3-/4-}$ redox system. The cyclic voltammograms of 5 mM solutions of $[Fe(CN)_6]^{3-/4-}$, measured with all electrodes, describe a typical reversible redox process characteristic of $[Fe(CN)_6]^{3-/4-}$. Quantitative characteristics of the electrochemical impedance

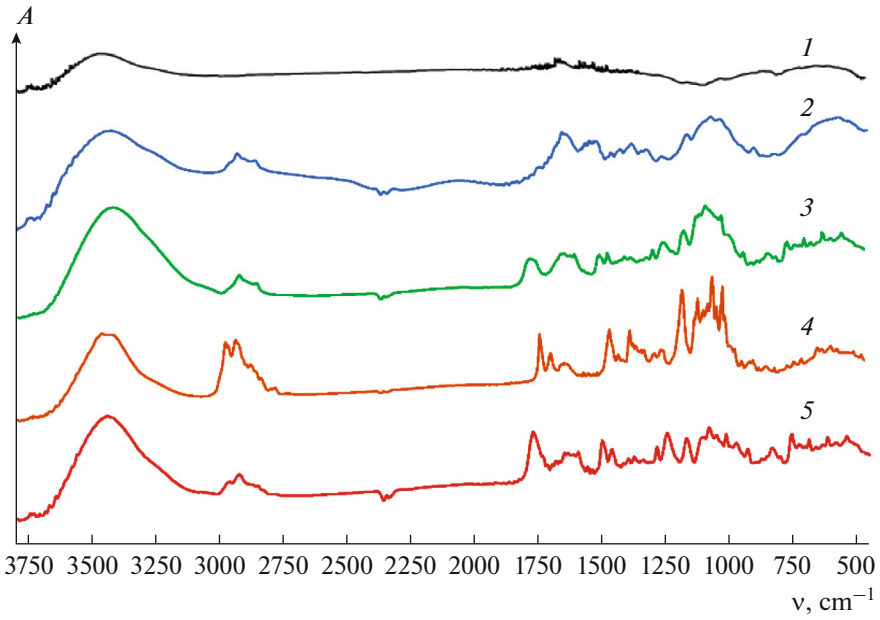

Fig. 2. IR spectra of (*1*) graphitized carbon black Carboblack C, (*2*) Carboblack C–chitosan composite, (*3*) polyarylene phthalide, (*4*) clarithromycin, and (*5*) polyarylene phthalide–clarithromycin complex.

spectra were determined using the equivalent Randles circuit (Fig. 3b, inset). The obtained values are presented in Table 1, where R_s and R_{et} represent solution resistance and charge transfer resistance, respectively, Q is the constant phase element, W is the Warburg impedance, and N is the roughness of the electrode surface [32]. The highest currents and, consequently, the lowest value of R_{et} were observed for the CB–CHT/GCE (Fig. 3, curve *2*) compared to the bare GCE (curve *1*). The lowest value of N for the CB–CHT-modified electrode indicates that its surface is the roughest, which is consistent with SEM images. The lowest currents and the highest R_{et} were observed for the PAP-modified GCE (curve *3*), confirming the necessity of using the CB–CHT modification. Upon the deposition of the polymeric PAP film on the CB–CHT/GCE (curve *4*), R_{et} increased and currents decreased compared to the bare GCE, indicating a decrease in the electron transfer rate for the $[Fe(CN)_6]^{3-/4-}$ redox couple. However, after the removal of clarithromycin from the polymer and the formation of the final sensor layer (curve *5*), R_{et} decreased, and currents reached values similar to those of the bare GCE. The electron transfer rate increased due to the formation of pores in the polymer, allowing $[Fe(CN)_6]^{3-/4-}$ ions to penetrate through the electrode surface. The decrease in N indicates that the electrode surface becomes rougher. After accumulating clarithromycin from a 0.3 mM solution (curve *6*), the peak currents in the CV decreases, and R_{et} increased, confirming the incorporation of clarithromycin.

Clarithromycin was detected using 5 mM $[Fe(CN)_6]^{3-/4-}$ as a probe, because the oxidation peak currents of clarithromycin itself were relatively low and did not allow the detection of clarithromycin with high sensitivity. The use of a probe typically significantly increases the sensitivity of voltammetric MIP sensors.

Table 1. Parameters of electrochemical impedance spectra for different stages of electrode modification in a 5 mM $[Fe(CN)_6]^{3-/4-}$ solution (0.1 M KCl, $n = 5$, $P = 0.95$)

Electrode	R_s, Ohm	Q, μS	N	R_{et}, Ohm	W, μS
GCE	107.7 ± 2.1	13.1 ± 0.7	0.96 ± 0.01	93.0 ± 3.8	427 ± 8
CB–CHT/CGE	102.3 ± 3.3	16.5 ± 1.0	0.76 ± 0.01	53.5 ± 3.6	367 ± 7
PAP/GCE	105.2 ± 5.6	10.2 ± 0.8	0.92 ± 0.03	208.3 ± 8.5	282 ± 9
PAP/CB–CHT/GCE	101.6 ± 6.1	12.2 ± 1.0	0.88 ± 0.02	126.4 ± 4.6	211 ± 6
miPAP/CB–CHT/GCE	104.6 ± 3.6	14.9 ± 0.7	0.83 ± 0.01	68.8 ± 3.8	403 ± 3
miPAP/CB–CHT/GCE after Clr accumulation (0.3 mM)	108.3 ± 3.8	13.5 ± 0.6	0.84 ± 0.02	145.5 ± 4.2	310 ± 6

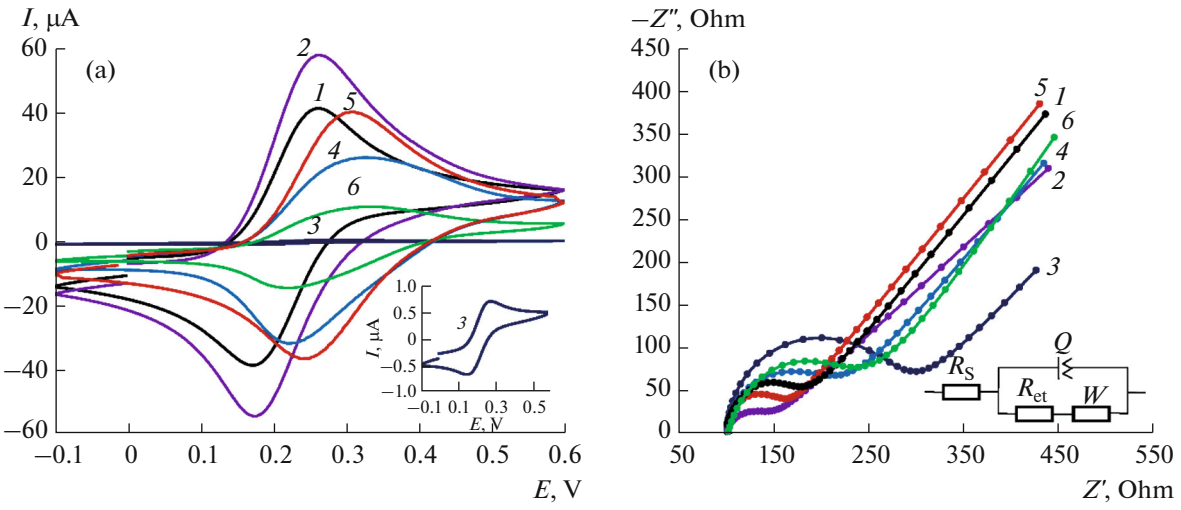

Fig. 3. (a) Cyclic voltammograms of 5 mM $[Fe(CN)_6]^{3-/4-}$ measured with (*1*) the GCE, (*2*) CB–CHT/GCE, (*3*) PAP/GCE, (*4*) PAP/CB–CHT/GCE, (*5*) miPAP/CB–CHT/GCE, and (*6*) miPAP/CB–CHT/GCE after accumulation of clarithromycin from a 0.3 mM solution; Inset: cyclic voltammograms at the PAP/GCE. (b) Nyquist diagrams of the corresponding electrodes.

With an increase in the concentration of clarithromycin, the oxidation peak current of $[Fe(CN)_6]^{4-}$ on a miPAP/CB–CHT/GCE (curve *4*) decreased, and the analytical signal was represented by the difference (ΔI_p) between the oxidation peak currents of $[Fe(CN)_6]^{4-}$ before and after clarithromycin incubation. Figure 4 shows differential pulse voltammograms of 5 mM $[Fe(CN)_6]^{3-/4-}$ obtained at different stages of GCE modification. The results correspond to the data from cyclic voltammetry and electrochemical impedance spectroscopy.

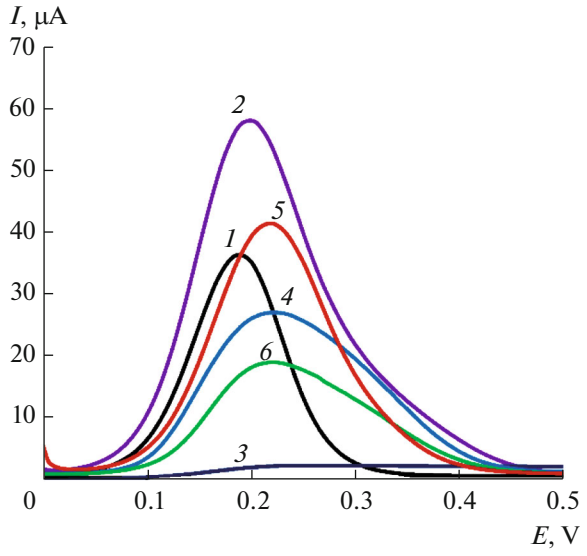

Fig. 4. Differential pulse voltammograms of 5 mM $[Fe(CN)_6]^{3-/4-}$ measured with (*1*) the GCE, (*2*) CB–CHT/GCE, (*3*) PAP/GCE, (*4*) PAP/CB–CHT/GCE, (*5*) miPAP/CB–CHT/GCE, and (*6*) miPAP/CB–CHT/GCE after accumulation of clarithromycin from a 0.3 mM solution.

To optimize the composition of the composite and the conditions for clarithromycin detection, we studied the dependences of the analytical signals and relative standard deviation on the amount of Carboblack C in the dispersion, the PAP-to-clarithromycin weight ratio in the polymer solution, template washing time from the PAP film, and incubation time of clarithromycin on a miPAP/CB–CHT/GCE before DPV measurements (Fig. 5). The results showed that an increase in the amount of Carboblack C in 1 mL of the dispersion with chitosan to 3 mg enhanced the oxidation peak currents of $[Fe(CN)_6]^{4-}$ (Fig. 5a), while the lowest relative standard deviations were observed at 1.5 and 2 mg of Carboblack B in the dispersion. This observation is presumably associated with the formation of a homogeneous and a stable layer of the CB–CHT composite. Therefore, the optimal amount of Carboblack C was selected at 2 mg. The dependence of ΔI_p on the PAP-to-clarithromycin ratio showed that the highest analytical signal and the lowest deviations were observed at a ratio of 10 : 4 (Fig. 5b). Complete template washing from the PAP film was achieved after 90 s of incubation in 1 M H_2SO_4 (Fig. 5c). The optimal incubation time of miPAP/CB–CHT/GCE in a 0.5 mM solution of clarithromycin was determined to be 40 s (Fig. 5d).

The linear relationship between the peak current and the concentration of clarithromycin in the solution was maintained in the concentration range 1×10^{-7}–5×10^{-4} M with a limit of detection of 5.3×10^{-8} M (Fig. 6). The linear dependences for nonimprinted polymer (NIP) sensors are shown in Fig. 5b. The presence of molecularly imprinted polymers sig-

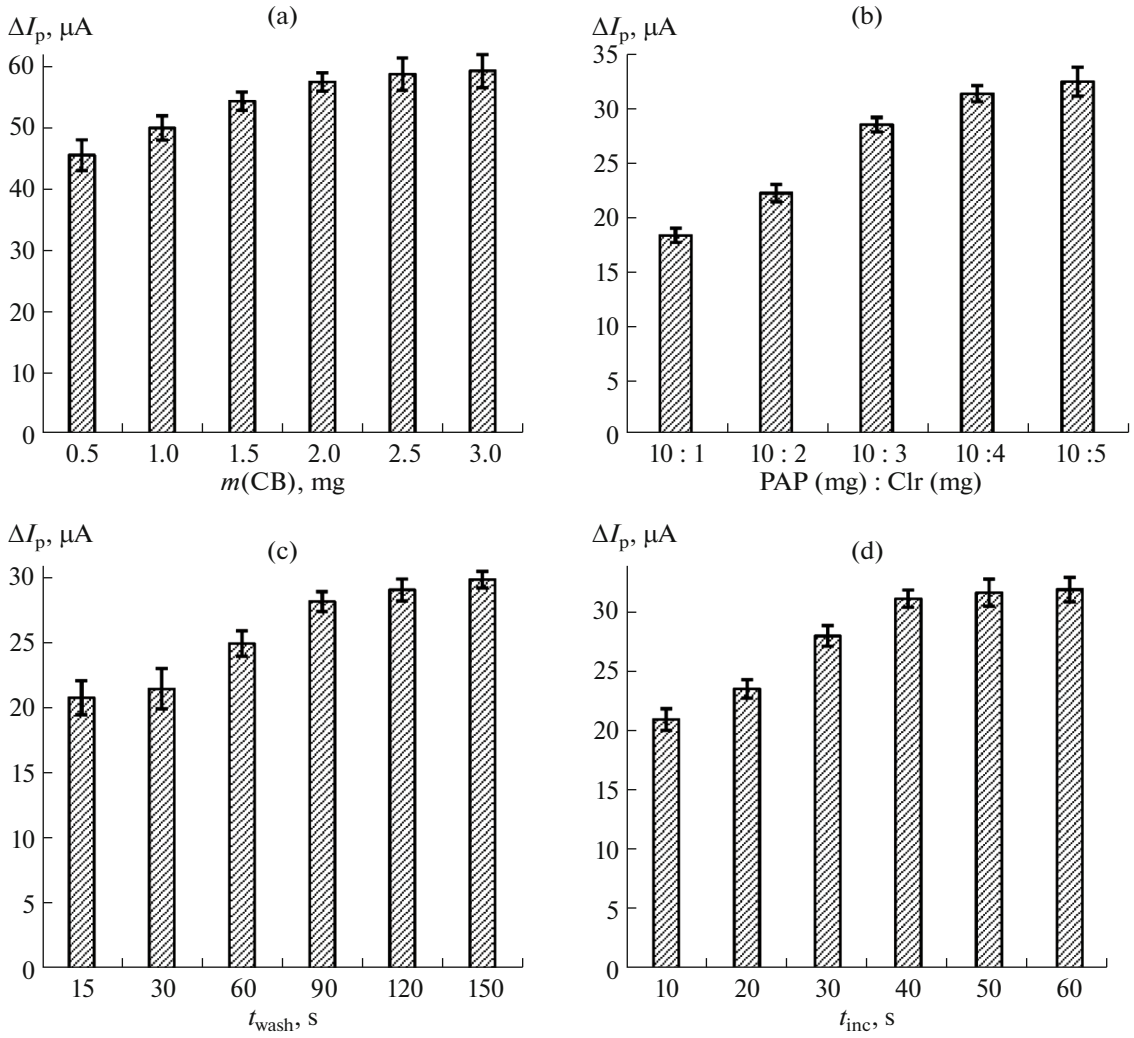

Fig. 5. (a) Dependence of the oxidation current of $[Fe(CN)_6]^{4-}$ at CB–CHT/GCE on the amount of graphitized carbon black Carboblack C in the dispersion. Dependences of ΔI_p (b) on the polyarylene phthalide-to-clarithromycin weight ratio in a polymer solution, (c) on the time of washing of the template from the polyarylene phthalide film, and (d) on the time of incubation of clarithromycin on miPAP/CB–CHT/GCE before recording differential pulse voltammograms ($n = 5$, $P = 0.95$).

nificantly enhances the sensitivity of the miPAP/CB–CHT/GCE, with an imprinting factor $F_{imp} = S_{MIP}/S_{NIP} = 9.88$. These results indicate the high sensitivity and selectivity of the miPAP/CB–CHT/GCE sensor.

The assessment of reproducibility and stability in clarithromycin determination with the miPAP/CB–CHT/GCE showed that, after ten consecutive measurements, the peak currents remained at 95.8% of the initial values with a relative standard deviation of 2.8%. After storage for 14 days at room temperature, the peak currents on the miPAP/CB–CHT/GCE were 93.7% of the initial value with a relative standard deviation of 3.9%.

To assess the accuracy of clarithromycin detection, the spike-recovery test was employed (Table 2), with the relative standard deviation not exceeding 2.1%. This indicates a good reproducibility of the results, while the recovery value of 98% attests to the high accuracy of the detection. To evaluate the analytical capabilities of the proposed sensor, it was tested for clarithromycin detection in human urine and blood plasma. The RSD for clarithromycin detection in urine and blood plasma were 5.8 and 9.3%, respectively, with recoveries of 96 and 90%. Higher errors in the clarithromycin detection in blood plasma are attributed to its complex composition and higher concentration of organic structures compared to urine. The sensor was also tested on food products (meat and milk). Here, we expected higher detection errors for clarithromycin due to the complex composition of the samples. The RSD for clarithromycin detection in meat and milk were 9.8 and 8.3%, respectively, with recoveries of 80 and 92%. However, these results can be considered acceptable and used for further analy-

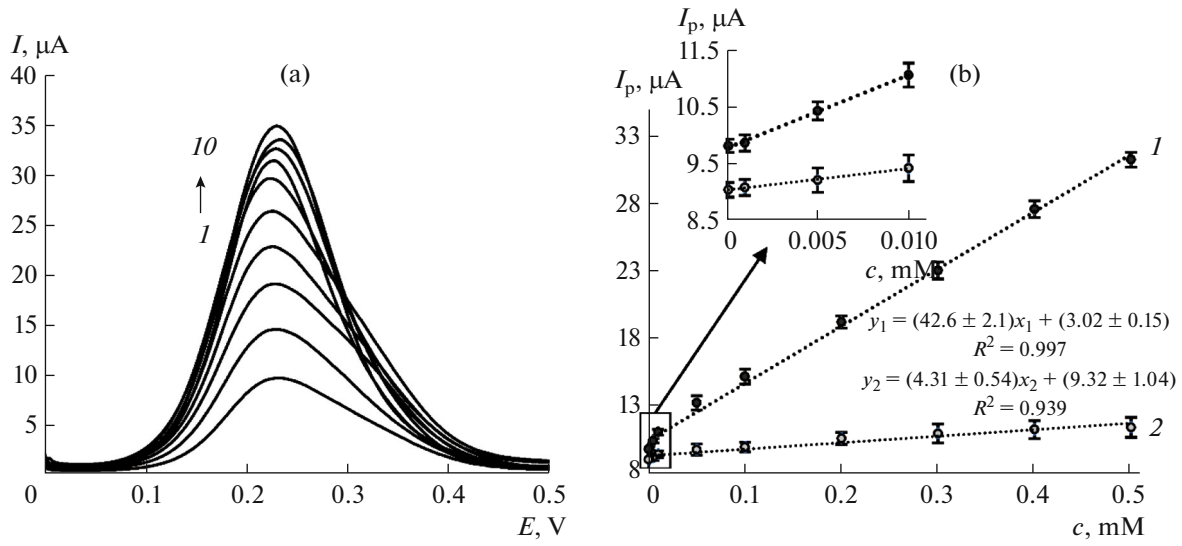

Fig. 6. (a) Differential pulse voltammograms of clarithromycin solutions of different concentrations ((*1*) 0.5, (*2*) 0.4, (*3*) 0.3, (*4*) 0.2, (*5*) 0.1, (*6*) 0.05, (*7*) 0.01, (*8*) 0.005, (*9*) 0.001, and (*10*) 0.0001 mM) measured with the miPAP/CB–CHT/GCE; (b) corresponding calibration plots for (*1*) the miPAP/CB–CHT/GCE and (*2*) niPAP/CB–CHT/GCE ($n = 5$, $P = 0.95$).

ses. The added clarithromycin concentrations in real samples were selected based on its potential presence according to the published data [33–35].

The main goal of developing a miPAP/CB–CHT/GCE was to enhance the sensor selectivity towards clarithromycin. To evaluate the effect on the analytical signal of clarithromycin, azithromycin (Azm) and lincomycin (Lin) antibiotics were selected. The DPV curves of azithromycin and lincomycin solutions at equal concentrations (0.5 mM) were recorded using $[Fe(CN)_6]^{3-/4-}$ as the probe under the same conditions. The miPAP/CB–CHT/GCE sensor exhibits the highest selectivity towards clarithromycin compared to azithromycin and lincomycin (Fig. 7). This can be attributed to the formation of more specific binding sites.

CONCLUSIONS

Thus, a highly selective voltammetric sensor for clarithromycin detection has been developed based on a GCE modified with a composite of chitosan, graphitized carbon black, and molecularly imprinted polyarylene phthalide. The MIP was obtained via phase inversion by solvent evaporation. A significant advantage of the sensor is its simple fabrication process using the dry phase inversion method. Scanning electron microscopy confirmed the formation of a homogeneous and a dense polymer film on the electrode surface, while the composite of chitosan and Carboblack C substantially enhanced peak currents. The optimal time for template washing and sensor incubation in the clarithromycin solution was determined to be 90 and 40 s, respectively. The developed sensor exhibits high selectivity towards the target antibiotic, and the presence of specific binding sites in the polymer film enables the detection of clarithromycin with sensitivity nearly ten times higher than that of a similar sensor without molecular imprints. Evaluation of selectivity towards other antibiotics (azithromycin and lincomycin) showed that the proposed sensor exhibits high selectivity towards clarithromycin. The obtained sensor was successfully applied to clarithromycin detection in biological fluids, meat, and milk samples, with recoveries ranging from 90 to 96, 80, and 92%, respectively, while RSD did not exceed 10% in all cases.

Table 2. Detection of clarithromycin by differential pulse voltammetry with the proposed sensor and $[Fe(CN)_6]^{3-/4-}$ as a probe (20 mV/s, $n = 5$, $P = 0.95$)

Sample	Added, μM	Found, μM	RSD, %	Recovery, %
PBS	0.50	0.49 ± 0.02	2.1	98
Urine	5.0	4.8 ± 0.3	5.8	96
Blood plasma	0.60	0.54 ± 0.08	9.3	90
Meat extract	0.10	0.08 ± 0.01	9.8	80
Milk	0.50	0.46 ± 0.07	8.3	92

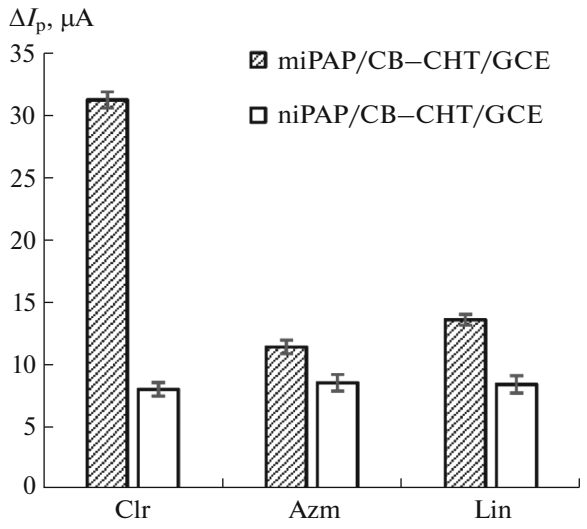

Fig. 7. Responses of the miPAP/CB–CHT/GCE and niPAP/CB–CHT/GCE to clarithromycin (0.5 mM), azithromycin (0.5 mM), and lincomycin (0.5 mM) ($n = 5$, $P = 0.95$).

ACKNOWLEDGMENTS

The authors are grateful to the Laboratory of Functional Polymer Synthesis at the Ural Federal Institute of Chemistry and Technology of the Russian Academy of Sciences, led by Dr. V.A. Kraikin, for providing the polymer samples.

FUNDING

The work was supported by the Russian Science Foundation (grant no. 21-73-00295, https://rscf.ru/en/project/21-73-00295/).

ETHICS APPROVAL AND CONSENT TO PARTICIPATE

All procedures performed in studies involving human participants were in accordance with the ethical standards of the institutional and/or national research committee and with the 1964 Helsinki Declaration and its later amendments or comparable ethical standards.

Informed consent was obtained from all individual participants involved in the study.

CONFLICT OF INTEREST

The authors of this work declare that they have no conflicts of interest.

REFERENCES

1. BelBruno, J., *Chem. Rev.*, 2019, vol. 119, p. 94. https://doi.org/10.1021/acs.chemrev.8b00171
2. Benachio, I., Lobato, A., and Gonçalves, L.M., *J. Mol. Recognit.*, 2021, vol. 34, p. 2878. https://doi.org/10.1002/jmr.2878
3. Crapnell, R.D., Hudson, A., Foster, C.W., Eersels, K., Grinsven, B., Cleij, T.J., Banks, C.E., and Peeters, M., *Sensors*, 2019, vol. 19, p. 204. https://doi.org/10.3390/s19051204
4. Wulff, G., *Microchim. Acta*, 2013, vol. 180, no. 15, p. 1359. https://doi.org/10.1007/s00604-013-0992-9
5. Yarkaeva, Y., Maistrenko, V., Dymova, D., Zagitova, L., and Nazyrov, M., *Electrochim. Acta*, 2022, vol. 433, p. 141222. https://doi.org/10.1016/j.electacta.2022.141222
6. Dmitrienko, E.V., Pyshnaya, I.A., Martyanov, O.N., and Pyshnyi, D.V., *Russ. Chem. Rev.*, 2016, vol. 85, p. 513. https://doi.org/10.1070/RCR4542
7. Poller, A.-M., Spieker, E., Lieberzeit, P.A., and Preininger, C., *ACS Appl. Mater. Interfaces*, 2017, vol. 9, p. 1129. https://doi.org/10.1021/acsami.6b13888
8. Dima, S.-O., Meouche, W., Dobre, T., Nicolescu, T.-V., and Sarbu, A., *React. Funct. Polym.*, 2013, vol. 73, p. 1188. https://doi.org/10.1016/j.reactfunctpolym.2013.05.014
9. Yang, Q., Wu, X., Peng, H., Fu, L., Song, X., Li, J., Xiong, H., and Chen, L., *Talanta*, 2018, vol. 176, p. 595. https://doi.org/10.1016/j.talanta.2017.08.075
10. Mulder, M., *Basic Principles of Membrane Technology*, Dordrecht: Kluwer, 1991.
11. Wang, H.Y., Kobayashi, T., and Fujii, N., *Langmuir*, 1996, vol. 12, p. 4850. https://doi.org/10.1021/la960243y
12. Noaman, U.H. and Park, J.K., *Polym. Compos.*, 2008, vol. 29, p. 949. https://doi.org/10.1002/pc.20479
13. Tasselli, F., Donato, L., and Drioli, E., *J. Membr. Sci.*, 2008, vol. 320, p. 167. https://doi.org/10.1016/j.memsci.2008.03.071
14. Silvestri, D., Barbani, N., Cristallini, C., Giusti, P., and Ciardelli, G., *J. Membr. Sci.*, 2006, vol. 282, p. 284. https://doi.org/10.1016/j.memsci.2006.05.031
15. Mkhize, D.S., Nyoni, H., Quinn, L.P., Mamba, B.B., and Msagati, T.A.M., *Environ. Sci. Pollut. Res. Int.*, 2017, vol. 24, p. 11694. https://doi.org/10.1007/s11356-017-8829-4
16. Kobayashi, T., Murawaki, Y., Reddy, P.S., Abe, M., and Fujii, N., *Anal. Chim. Acta*, 2001, vol. 435, p. 141. https://doi.org/10.1016/S0003-2670(00)01281-2
17. Qiu, Z., Fan, D., Xue, X., Guo, S., Lin, Y., Chen, Y., and Tang, D., *Chemosensors*, 2022, vol. 10, p. 252. https://doi.org/10.3390/chemosensors10070252
18. Reddy, P.S., Kobayashi, T., Abe, M., and Fujii, N., *Eur. Polym. J.*, 2002, vol. 38, p. 521. https://doi.org/10.1016/S0014-3057(01)00212-9
19. Abdel-Shafy, H.I., Sayour, H.E., and Mansour, M.S.M., *Polym. Adv. Technol.*, 2016, vol. 27, p. 724. https://doi.org/10.1002/pat.3704
20. Donato, L., Tasselli, F., and Drioli, E., *Sep. Sci. Technol.*, 2010, vol. 45, p. 2273. https://doi.org/10.1080/01496395.2010.510089

21. Barbani, N., Rosellini, E., Donati, M., Costantino, P., Cristallini, C., and Ciardelli, G., *Polym. Int.*, 2017, vol. 66, p. 900. https://doi.org/10.1002/pi.5334
22. Ciobanu, M., Marin, L., Cozan, V., and Bruma, M., *Rev. Adv. Mater. Sci.*, 2009, vol. 22, p. 89.
23. Kraikin, V., Fatykhov, A., Gileva, N., Kravchenko, A., and Salazkin, S., *Magn. Reson. Chem.*, 2020, vol. 59, no. 1, p. 61. https://doi.org/10.1002/mrc.5079
24. Salazkin, S., Shaposhnikova, V., Machulenko, L., Gileva, N., Kraikin, V., and Lachinov, A., *Polym. Sci., Ser. A*, 2008, vol. 50, no. 3, p. 243. https://doi.org/10.1134/S0965545X08030024
25. Gileva, N., Kraikin, V., Sedova, E., Lobov, M., Kuznetsov, S., and Salazkin, S., *Russ. J. Appl.Chem.*, 2005, vol. 78, no. 10, p. 1683. https://doi.org/10.1007/S11167-005-0586-3
26. Salikhov, R., Zilberg, R., Mullagaliev, I., Salikhov, T., and Teres, Y., *Mendeleev Commun.*, 2022, vol. 32, p. 520. https://doi.org/10.1016/j.mencom.2022.07.029
27. Yarkaeva, Y., Maistrenko, V., Zagitova, L., Nazyrov, M., and Berestova, T., *J. Electroanal. Chem.*, 2021, vol. 903, p. 115839. https://doi.org/10.1016/j.jelechem.2021.115839
28. Zagitova, L., Yarkaeva, Y., Zagitov, V., Nazyrov, M., Gainanova, S., and Maistrenko, V., *J. Electroanal. Chem.*, 2022, vol. 992, p. 116774. https://doi.org/10.1016/j.jelechem.2022.116744
29. Jafari, S., Dehghani, M., Nasirizadeh, N., and Azimzadeh, M., *J. Electroanal. Chem.*, 2018, vol. 829, p. 27. https://doi.org/10.1016/j.jelechem.2018.09.053
30. Shenderovich, V.A., Pasternak, N.A., Stolyarova, L.G., Solov'eva, V.E., Vlasova, I.V., Ved'mia, E.A., Sheveleva, S.A., *MUK 4.2.026-95: Rapid Method for Determining Antibiotics in Food Products*, Moscow, 1995.
31. Jafari, M., Tashkhourian, J., and Absalan, G., *Talanta*, 2018, vol. 178, p. 870. https://doi.org/10.1016/J.TALANTA.2017.10.005
32. Lasia, A., *Electrochemical Impedance Spectroscopy and Its Applications*, New York: Springer, 2014. https://doi.org/10.1007/978-1-4614-8933-7
33. Kul, A., Ozdemir, M., and Sagirl, O., *J. Pharm. Biomed. Anal.*, 2022, vol. 208, p. 114438. https://doi.org/10.1016/j.jpba.2021.114438
34. Chu, S.-Y., Sennello, L.T., and Sonders, R.C., *J. Chromatogr. B: Biomed. Sci. Appl.*, 1991, vol. 571, nos. 1–2, p. 199. https://doi.org/10.1016/0378-4347(91)80446-J
35. Zuckerman, J.M., Qamar, F., and Bono, B.R., *Med. Clin. North Am.*, 2011, vol. 95, no. 4, p. 761. https://doi.org/10.1016/j.mcna.2011.03.012

Translated by O. Zhukova